Available online at www.sciencedirect.com
ScienceDirect
Ceramics International 36 (2010) 847–853
CERAMICS INTERNATIONAL
www.elsevier.com/locate/ceramint

Synthesis and characteristics of nanocrystalline 3Y-TZP and CuO powders for ceramic composites

Louis Winnubst [a,*], Peter J. de Veen [b], Shen Ran [b], Dave H.A. Blank [b]

[a] *Inorganic Membranes, Membrane Technology Group, University of Twente, P.O. Box 217, 7500 AE Enschede, The Netherlands*
[b] *Inorganic Materials Science, Faculty of Science and Technology and MESA+ Institute for Nanotechnology, University of Twente, P.O. Box 217, 7500 AE Enschede, The Netherlands*

Received 21 August 2009; received in revised form 26 August 2009; accepted 29 August 2009
Available online 29 October 2009

Abstract

A weakly agglomerated 3Y-TZP powder with 100% tetragonal crystal structure and a primary crystallite diameter of 8 nm was prepared by co-precipitation of metal chlorides in an ammonia solution, followed by extensive washing with ethanol, drying and calcining at 550 °C. Powder characteristics as function of thermal treatment are discussed. A copper oxalate precipitation for the preparation of nanocrystalline CuO powders was optimised in order to minimise aggregation and agglomeration. The influence of calcination procedure and synthesis medium on several powder characteristics of the CuO powders were investigated in detail. Oxalate precipitation in ethanol followed by sequential drying and calcination in air at 250 °C in an open tubular furnace with proper air-powder contact area was found to be the optimal procedure for producing nanocrystalline single-phase CuO powder with small aggregates and weak agglomerates. With this optimal procedure a CuO powder with crystallite diameter and BET equivalent particle diameter of respectively 12 and 20 nm was obtained.

Keywords: A. Powders: chemical preparation; A. Calcination; D. Y_2O_3–ZrO_2; CuO, Nano-powder

1. Introduction

Ceramic materials with grain sizes in the submicrometer (<0.5 μm) range, so called nanostructured ceramics, have attracted great interest due to their special properties. In these materials a significant atom fraction is situated in the grain-boundary region. Generally grain boundaries show metastabilities and therefore nanostructured ceramics can give special material properties which are not found in coarser grained systems [1]. It has been shown in many papers that sintering temperature for ceramics can be lowered by several hundred degrees by reducing the starting particle size to the nanometre range [2–4]. Nanostructured zirconia ceramics were also reported to possess very good mechanical properties [5] strongly enhanced superplastic behaviour for, e.g. near net-shape forming [6,7], and improved wear-resistance under dry sliding conditions [8]. It can also be used as interlayer for ceramic–ceramic bonding at lower temperature [9].

Coarse-grained CuO doped 3Y-TZP composite ceramics produced from submicron starting powders have shown promising low friction coefficient under dry sliding conditions [10] and enhanced superplastic behaviour [11]. It is of great interest to examine how the grain size influences the properties of these CuO doped 3Y-TZP composites, especially when the grain size is in the nanometre range.

In order to obtain a nanostructured composite ceramic with special properties, ultra-fine grained starting powders are of course required. Fabrication of nanocrystalline 3Y-TZP powders has been extensively investigated in the past two decades [12–16]. It was reported that a weakly agglomerated 3Y-TZP powder with a primary crystallite diameter of 8 nm can be successfully synthesised by co-precipitation of chlorides in an ammonia solution followed by extensive washing with ethanol [15,16]. The washing steps are critical for agglomeration control. In this paper the 3Y-TZP nano-powders were produced by this technique. A copper oxalate precipitation technique is often used to prepare CuO catalysts with crystallite

* Corresponding author. Tel.: +31 53 489 2994; fax: +31 53 489 4611.
E-mail address: a.j.a.winnubst@utwente.nl (L. Winnubst).

0272-8842/$36.00
doi:10.1016/j.ceramint.2009.08.001

sizes in the nanometre range [17–18]. However the important characteristics necessary for ceramic fabrication of this CuO powder, like degree of aggregation and agglomeration, cannot be found in literature.

The work presented in this paper was undertaken to optimise the copper oxalate precipitation procedure from the ceramic fabrication point of view. Emphasis is laid on reduction of aggregates and agglomerates. The fabrication, details on calcination behaviour and powder characteristics (aggregation/agglomeration) of nanocrystalline 3Y-TZP powders are described as well.

2. Experimental

2.1. Preparation of 3Y-TZP powder

A nanocrystalline powder of 3 mol% yttria-stabilized tetragonal zirconia polycrystals (3Y-TZP) was prepared by co-precipitation an aqueous solution (1.2 M; pH ∼ 2) of $ZrOCl_2{\cdot}8H_2O$ (Merck Chemical, Germany) and YCl_3 (Aldrich Chemical, Germany). Using a peristaltic pump the solution was added to concentrated aqueous ammonia (pH ∼ 14) at 3.5 ml min^{-1} in a Teflon®-coated steel vessel provided with a top-mounted turbine stirrer. More details on equipment and experimental conditions are given in [16,19,20]. The resulting wet gel was washed with copious amounts of water/ammonia mixtures, until the decanted clear liquid no longer became turbid upon addition of 0.1 M $AgNO_3$, indicating that the system was chloride-free. Subsequently the precipitate was washed with ethanol to remove water. Ethanol washing was undertaken until the density of the decanted liquid was less than 0.79 g cm^{-3}, implying the water content is less than 5%. After the liquid in the suspension was filtered out, the remaining wet gel was oven-dried overnight at 100 °C. The resulting amorphous yttrium–zirconium hydroxide powder was ground and sieved through a 180 μm sieve, and subsequently calcined at 550 °C in stagnant air for 2 h. The calcined powder was ground and sieved again, and stored in a desiccator. This 3Y-TZP powder is denoted as CP 3Y-TZP powder hereafter.

2.2. Preparation of CuO powder

A copper oxalate precipitation method in ethanol or water was performed to prepare the nanocrystalline copper-oxide powders. $Cu(NO_3)_2{\cdot}3H_2O$ (Merck Chemical, Germany) and oxalic acid ($H_2C_2O_4{\cdot}2H_2O$, Merck Chemical, Germany) were separately dissolved into either ethanol or water to form a 0.5 M solution. In order to make sure that all Cu^{2+} ions precipitate, an excess of 5 mol% oxalic acid was used. The copper nitrate solution was slowly added to the oxalic acid solution under vigorously stirring and a light blue complex precipitate of copper oxalate was formed. After addition of the Cu solution the suspension was stirred for an extra 30 min. The suspension prepared in ethanol was subsequently oven-dried at 100 °C for 24 h. The suspension prepared in water was washed with water and ethanol prior to drying (100 °C for 24 h). For comparison, part of the suspension prepared in water was dried without further washing. The dried cakes were ground slightly in a plastic mortar and sieved through a 180 μm sieve. Copper-oxide powders were obtained by thermal decomposition of the copper oxalate powders at 250, 300 and 450 °C respectively for 2 h. The resulting powders were sieved again and stored in a desiccator prior to use.

2.3. Characterisation

X-ray diffraction (XRD, X'pert_APD, PANalytical, Cu-$K_{\alpha 1}$, λ = 1.542 Å) was used to analyze the crystal structure of the 3Y-TZP and CuO powders and the primary crystallite size of those powders. The primary crystallite size (D_{XRD}) was calculated by the X-ray line broadening technique (XRLB), according to Scherrer's equation:

$$D_{XRD} = \frac{K \cdot \lambda}{\beta \cos\theta} \quad (1)$$

where K is the Scherrer constant; λ is the wavelength of the X-ray in nm; β is the line broadening; θ is the Bragg angle.

The relative amount of CuO, Cu_2O and Cu-metal phase in the copper-oxide powders were estimated by the relative intensity ratio of the peaks of the XRD patterns. A high-temperature XRD measurement was conducted on the as-dried yttrium–zirconium hydroxide powder in order to obtain an indication of the temperature at which amorphous zirconia–yttria transforms to crystalline 3Y-TZP.

Specific surface areas of all powders were determined by the BET method (ASAP 2400, Micromeritics). From the BET specific surface area an equivalent spherical particle diameter (D_{BET}) was calculated by:

$$D_{BET} = \frac{6}{S_{BET} \cdot \rho} \quad (2)$$

where S_{BET} is the BET surface area and ρ is the theoretical density of the material.

Thermal gravimetric and differential scanning calorimetric techniques (TGA/DSC, Setaram Setsys 16) were used to investigate crystallization behaviour of the amorphous yttrium–zirconium hydroxide powder as well as thermal decomposition behaviour of copper oxalate powders. Transmission electron microscope (TEM, CM30 Twin/STEM, Philips) was used to study the morphology of the 3Y-TZP and CuO powders. Morphologies of the copper oxalate and CuO powders were also observed by scanning electron microscopy (SEM-EDX, Thermo NORAN Instruments).

3. Results and discussion

3.1. Characteristics of 3Y-TZP powder

DSC analysis on the co-precipitated yttrium–zirconium hydroxide powder shows an exothermic signal at around 460 °C (Fig. 1), which can be ascribed to the crystallization of the amorphous hydroxide precipitate. In accordance with this DSC result, high-temperature XRD analysis shows that the yttrium–

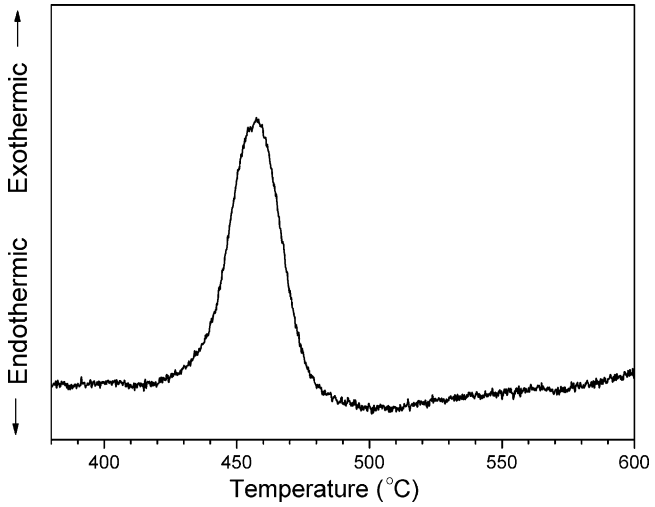

Fig. 1. DSC of co-precipitated yttrium–zirconium hydroxide.

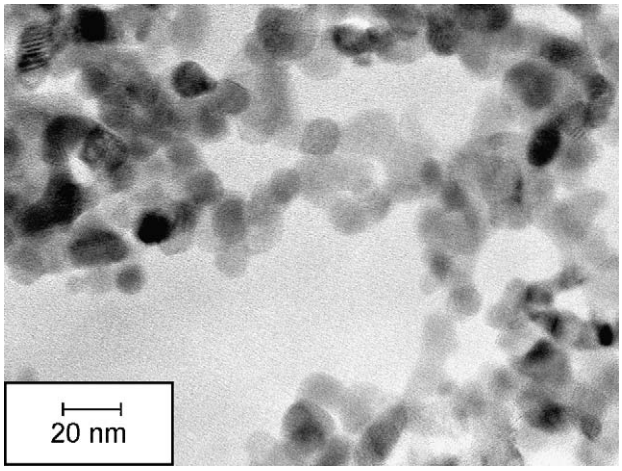

Fig. 3. TEM image of 3Y-TZP powder prepared by co-precipitation, calcined at 550 °C for 2 h.

zirconium hydroxide powder remains amorphous when calcined at temperatures ≤400 °C and exhibits a tetragonal crystal structure after calcination at 500 °C (Fig. 2). In order to ensure complete crystallization for CP 3Y-TZP powders, calcination at 550 °C for 2 h was used for further material characterisation. The crystallite size (D_{XRD}) of the tetragonal 3Y-TZP powder as calcined at 550 °C is 8 nm. Particle size as calculated from the BET surface area (S_{BET} = 106 $m^2\,g^{-1}$; D_{BET}) is 10 nm by using Eq. (2). The good agreement between the values of D_{XRD} and D_{BET} indicates a low degree of aggregation in this CP 3Y-TZP powder.

More details on morphology of crystallites and aggregates in the CP 3Y-TZP powder is revealed by TEM (Fig. 3), showing uniform crystallites with a size of less than 10 nm, which is in good agreement with the crystallite size value as determined by the XRLB method (D_{XRD}). These crystallites are arranged in strings of small aggregates. In Ref. [2] the sintering behaviour of an isostatically pressed CP 3Y-TZP compact was compared with a compact of the well-known TOSOH TZ3Y powder (D_{XRD} = 34 nm; D_{BET} = 47 nm), showing that the nanocrystalline CP 3Y-TZP sample was dense after sintering at 1050 °C for 7 h (grain size: 60 nm) while for the TOSOH powder compact a sintering temperature of 1350 °C (3 h) was necessary with a resulting grain size of 350 nm.

3.2. Thermal decomposition of copper oxalate

Thermal decomposition of copper oxalate powders is depicted in Fig. 4. The copper oxalate loses about 3% of its weight between 30 and 250 °C due to desorption of adsorbed water and gases. Between 250 and 310 °C a weight loss of almost 50 wt% is observed, combined with an exothermic signal in DSC. Obviously this exothermic reaction is the decomposition of copper oxalate by release of CO and CO_2. It is known from literature that in this temperature range copper oxalate decomposes into copper metal by a stepwise cation reduction ($Cu^{2+} \rightarrow Cu^{+} \rightarrow Cu^{0}$) [18,21], which causes the large weight loss. In our case this weight loss is immediately followed by a (small) weight gain, indicating that the Cu resulted from the decomposition of copper oxalate powder re-oxidises to CuO.

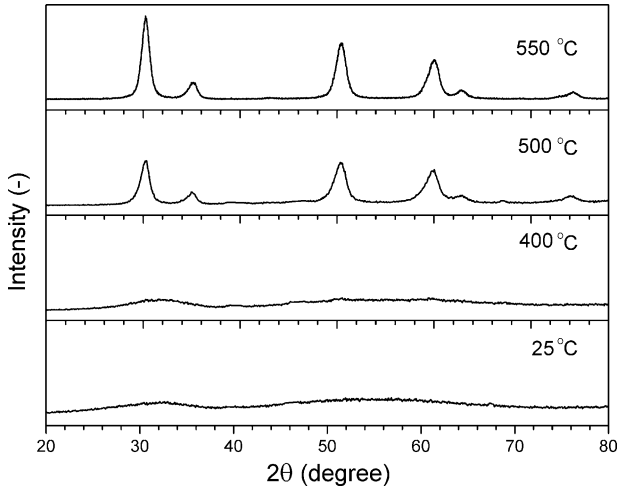

Fig. 2. XRD patterns of co-precipitated 3Y-TZP powder calcined at various temperatures.

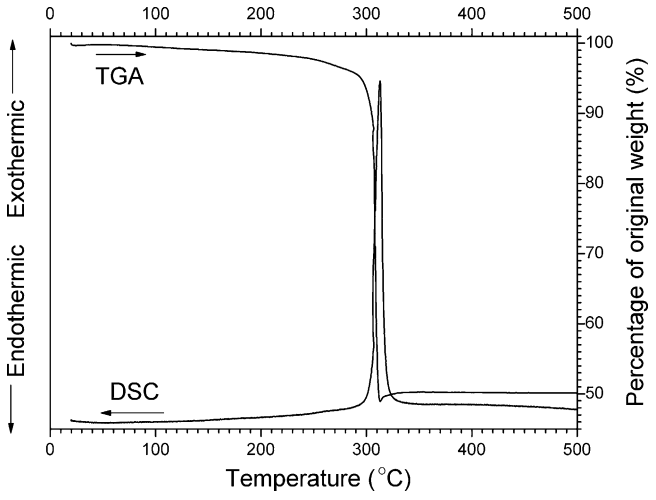

Fig. 4. Thermal decomposition of copper oxalate as measured by TGA/DSC.

Table 1
Powder characteristics of CuO prepared via decomposition of copper oxalate.

ID	Calc. T (°C)	D_{XRD} (nm)	S_{BET} ($m^2\ g^{-1}$)	D_{BET} (nm)	n	q	D_{agg} (nm)
CuO-360	450	50	2.7	360	200	90	280
CuO-60	300	*N*	16	60	*N*	*N*	*N*
CuO-50	250	15	20	50	50	25	55
CuO-20	250[a]	12	45	20	25	15	30

Calc. T: calcination temperature; D_{XRD}: crystallite size determined by XRLB (Eq. (1)); D_{BET}: BET equivalent particle size (Eq. (2)); n: number of necks in an aggregate (Eq. (3)); q: number of particles in an aggregate, assuming simple cubic particle stacking; D_{agg}: average size of an aggregate (Eq. (4)); *N:* not measured;
[a] This powder was calcined at 250 °C in a tubular furnace.

3.3. Influence of calcination procedure on crystallite and aggregate size of CuO powders

Table 1 shows data from calcined powders of copper oxalate complexes prepared in an ethanol solution. Calcination was conducted in a room furnace except the one marked as 250[a], which was conducted in an open tubular furnace. The powders are classified (=ID) based on the particle diameter calculated from BET surface area (D_{BET}). As can be seen from this table the calcination procedure has a strong influence on the characteristics of the resulting copper-oxide powder. First of all the crystallite size (as determined by XRLB technique, D_{XRD}) increases strikingly with increasing calcination temperature. D_{XRD} of the 450 °C calcined copper-oxide powder (CuO-360) is more than three times larger than the 250 °C calcined one (respectively 50 and 15 nm). The particle diameter as calculated from BET surface area (D_{BET}) shows an even stronger dependence on calcination temperature. When calcination temperature increases from 250 to 450 °C the D_{BET} value increases more than six times (50 for the 250 °C calcined compared to 360 nm for the 450 °C calcined). The difference in furnace type also shows some influence on the powder characteristics. When an open tubular furnace is used for calcination, a CuO powder with smaller D_{XRD} (12 nm) and D_{BET} (20 nm) was obtained by calcining the powder at 250 °C.

The difference between D_{BET} and D_{XRD} values can be explained by the fact that in these powders the primary crystallites are clustered to aggregates. In these aggregates some spaces, for instance, the closed pores and the very narrow space close to the neck area of two crystallites, are not accessible for the adsorbent used in the BET experiments (N_2 in the current case). Thus the adsorbent cannot cover the crystallite surface completely. The difference between D_{BET} and D_{XRD} values is an indication of the degree of powder aggregation. According to Avery and Ramsay [22] the size and structure of aggregates are determined by the number of necks:

$$n = \frac{2D_{XRD}}{D_{N_2}}\left(1 - \frac{S_{BET}}{S_T}\right) \quad (3)$$

where n is the number of necks; D_{N_2} is the diameter of the adsorbent molecule used in BET measurement, i.e. 0.43 nm for N_2; S_{BET} is the measured BET surface area; and S_T is the theoretical surface area when it is assumed that each individual (spherical) crystallite is completely covered with adsorbent (so assuming a non-aggregated powder). From the number of necks the number of crystallites per aggregate, q, and subsequently the average size of the aggregates (D_{agg}) can be estimated for a certain packing structure of the aggregates. Here, for calculating q it is assumed that the crystallites in the aggregates have a simple cubic packing. The size of an aggregate (D_{agg}) consisting of q crystallites can then be estimated by the following equation, assuming all aggregates are spherically shaped with a uniform diameter D_{XRD}:

$$D_{agg} = \left(\frac{q}{1-p}\right)^{1/3} D_{XRD} \quad (4)$$

For a simple cubic packing of spherical particles the porosity $p = 0.476$.

As revealed by the n, q and D_{agg} values, the copper-oxide powder calcined at 450 °C in a room furnace shows a significant degree of aggregation (see Table 1). Aggregates in this powder consist of about 90 primary crystallites and have an average diameter close to 300 nm. For the powder calcined at 250 °C in a room furnace the degree of powder aggregation is remarkably reduced, as indicated by the D_{agg} of 55 nm and q of 25. After calcining the copper oxalate in an open-ended tubular furnace at 250 °C, the aggregation is even more inhibited (D_{agg} = 30 nm; q = 15). It can easily be calculated that the aggregate volume of the CuO-360 is around 1000 times larger than that in CuO-20.

The difference in crystallite size and especially the difference in degree of aggregation between the powders calcined in closed room furnace and open tubular furnace is likely to be caused by the actual cooling rate. Although a cooling rate of 2 °C min^{-1} was set in the ramp program, the room furnace cooled down much slower than the tubular furnace (~0.2 °C min^{-1} compared with 1 °C min^{-1}), because of furnace isolation. Therefore the powder was kept at relatively high-temperature for longer time in the room furnace, which means more crystallite and aggregate growth.

For ceramic fabrication, large aggregates are normally unfavourable because they give rise to large voids and poor uniformity in green powder compacts. From this point of view, calcination at 250 °C in an open tubular furnace is the optimal procedure. Fig. 5 shows a TEM image of the CuO powder prepared by this procedure, i.e. CuO-20. It is confirmed by this figure that the CuO-20 powder consists of crystallites with an average diameter around 10 nm showing only a small degree of aggregation.

3.4. Influence of calcination procedure on phase composition of CuO powders

The phase composition of copper-oxide powders calcined under different conditions was determined by XRD (see Fig. 6). Phase contents (in vol.%) were quantitatively estimated on the basis of the intensity ratios of the most intense XRD signal of

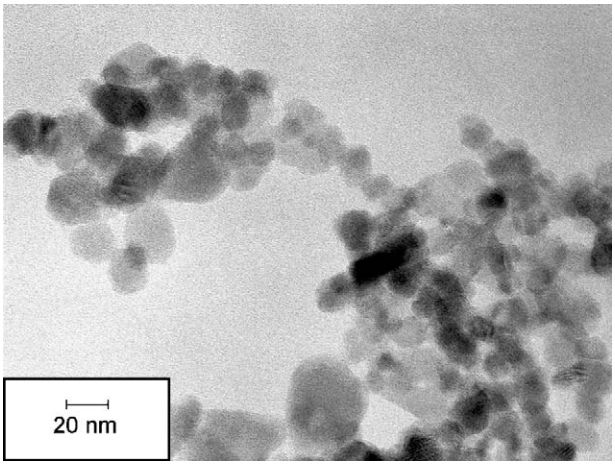

Fig. 5. TEM image of CuO-20 powder, which was prepared by oxalate precipitation followed by calcination at 250 °C in an open tubular furnace.

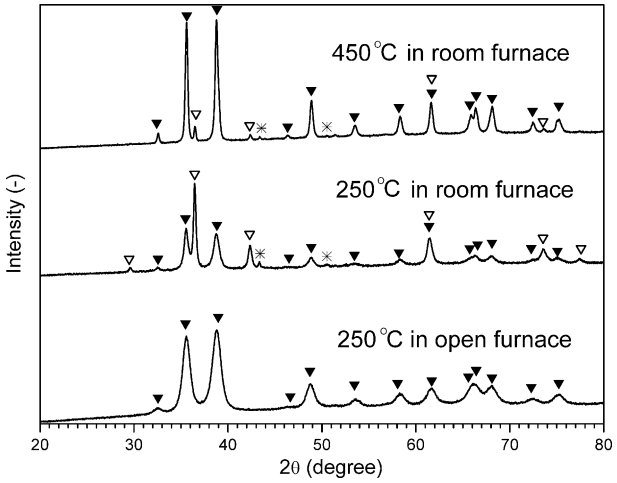

Fig. 6. XRD patterns of copper-oxide powders prepared by oxalate precipitation techniques, after calcining under different conditions. (▼) CuO; (▽) Cu_2O; (*) Cu.

each phase (see Table 2). After calcination at 250 °C in a room furnace, the copper-oxide powder consists of 50 vol.% of Cu_2O and 3 vol.% of metallic Cu because of an incomplete re-oxidation process. Calcination at 450 °C in a room furnace improves the oxidation reaction but still small amounts of Cu_2O and Cu phase are left. However, when an open-ended (tubular) furnace is used, the CuO exhibits a pure CuO phase after calcination at 250 °C for 2 h. In the case of calcination in the tube furnace, the powder is accessible for more fresh air if compared with a room furnace. It can be concluded that exposing the powder to fresh air during calcination is more favourable for obtaining a pure CuO phase.

Table 2
Phase composition in copper-oxide powders.

ID	Calcination T (°C)	Phase composition (vol.%)		
		CuO	Cu_2O	Cu
CuO-360	450	93	6	1
CuO-50	250	47	50	3
CuO-20	250[a]	100	0	0

[a] This powder was calcined at 250 °C in a tubular furnace (the other two in a room furnace).

Table 3
D_{BET} of CuO powder prepared with different oxalate precipitation and subsequent washing conditions.

ID	Precipitation solvent	Ethanol washing	D_{BET} (nm)[a]
CuO-E	Ethanol	No	20
CuO-W	Water	No	120
CuO-WE	Water	Yes	20

[a] All powders were calcined at 250 °C for 2 h in an open tubular furnace.

3.5. Influence of precipitation and washing medium on CuO powder characteristics

In the previous sections the characteristics of the CuO system are discussed for powders as prepared by precipitation and washing in ethanol. In this section the influence of precipitation and washing medium will be discussed. Table 3 shows D_{BET} of CuO powders prepared by precipitation in water or ethanol, while a part of the oxalate complex as precipitated in water was washed with ethanol to replace the liquid medium before drying. All powders were calcined in a tubular furnace at 250 °C for 2 h with heating and cooling rate of 2 °C min^{-1}. Sample CuO-E in Table 3 is therefore identical to CuO-20 as given in Tables 1 and 2.

The CuO powder possesses a D_{BET} of 120 nm when water is used as solvent during copper oxalate precipitation and no ethanol washing is applied. In contrast, if the copper oxalate prepared in water is afterwards thoroughly washed with ethanol, the CuO powder exhibits an identical D_{BET} after calcination as the one prepared by using ethanol as solvent during the whole process (20 nm, CuO-20). Reduction in aggregate size and/or agglomerate strength as caused by ethanol washing is generally ascribed to a lower surface tension of ethanol than that of water, which causes a lower particle packing during the drying process [23,24].

SEM images of dried copper oxalate powders prepared by precipitation in water without (Fig. 7a) and with (Fig. 7b) subsequent ethanol washing confirm the strong influence of washing medium on agglomerate structure: washing with ethanol results in a porous structure, whereas, the unwashed one shows denser agglomerates. After calcination a dense agglomerate structure is obtained after calcination copper oxalate, precipitated in water without subsequent ethanol washing (see Fig. 7c). On the other hand the ethanol-washed oxalate precipitate shows agglomerates (in a size of several μm) consisting of a porous packing of primary crystallites (or aggregates, see Fig. 7d), which are identical to the one prepared without involvement of any water.

The larger aggregates and the stronger agglomerates in the CuO powder produced without the ethanol washing step are difficult to break down during wet-milling or ultrasonic treatments. If this type of CuO powder is used for ceramic

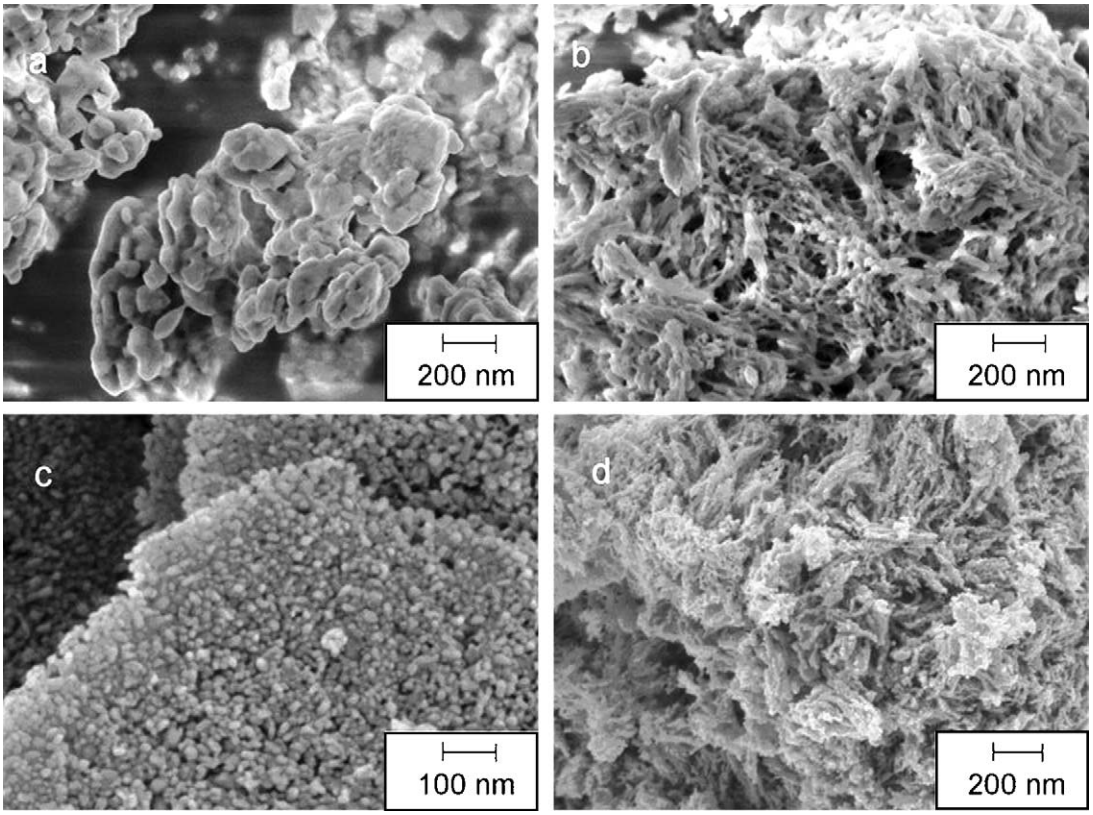

Fig. 7. SEM images of copper oxalate prepared by precipitation in water; (a and b) dried precipitates; (c and d) precipitates calcined at 250 °C for 2 h in an open tubular furnace; (a and c) no ethanol washing after precipitation (CuO-W); (b and d) precipitates were washed with ethanol (CuO-WE).

fabrication, large voids or significant inhomogeneities in the material could arise from the presence of such aggregates and agglomerates.

In Ref. [25] the sintering behaviour of an isostatically pressed CP 3Y-TZP compact was compared with a nano-composite containing 8 mol % CuO-50, showing a much faster densification of the nano-composite. A composite compact reached more than 95% relative density after (fast) heating at 15 °C min^{-1} to 1050 °C and immediate cooling to room temperature. Even a dense composite was obtained after sintering a powder compact at 960 °C for 20 h (heating rate 20 °C min^{-1}). This material had a nanostructured microstructure consisting of uniformly small grains of 120 nm [25].

4. Conclusions

An almost non-aggregated 3Y-TZP powder with a purely tetragonal crystal structure and an average crystallite size of 8 nm was prepared by co-precipitation of metal chlorides followed by calcination at 550 °C for 2 h. Nanocrystalline CuO powders were successfully produced by precipitation of copper oxalate followed by a thermal decomposition. The crystallite and aggregate size strongly increase with increasing calcination temperature. The type of furnace used for calcination slightly influences the aggregate size and affects the phase composition in the CuO powder. In order to obtain a CuO powder with small aggregates and weak agglomerates, calcination at 250 °C in an open-ended tubular furnace with good air-powder contact is recognised as the optimal thermal decomposition procedure. It is necessary to precipitate the oxalate complex in ethanol or to wash the precipitate in ethanol for obtaining these nano crystalline CuO powders with small aggregate size and weak agglomerates.

Acknowledgement

Dutch Technology Foundation (STW) is gratefully acknowledged for the financial support.

References

[1] J.R. Groza, Nanosintering, Nanostruct. Mater. 12 (5–8) (1999) 987–992.
[2] G.S.A.M. Theunissen, A.J.A. Winnubst, A.J. Burggraaf, Sintering kinetics and microstructure development of nanoscale Y-TZP ceramics, J. Eur. Ceram. Soc. 11 (4) (1993) 315–324.
[3] P. Duran, M. Villegas, J.F. Fernandez, F. Capel, C. Moure, Theoretically dense and nanostructured ceramics by pressureless sintering of nanosized Y-TZP powders, Mater. Sci. Eng. A 232 (1–2) (1997) 168–176.
[4] Q.S. Zhu, B. Fan, Low temperature sintering of 8YSZ electrolyte film for intermediate temperature solid oxide fuel cells, Solid State Ionics 176 (9–10) (2005) 889–894.
[5] G.F. Lange, Transformation toughening. 1. Size effects associated with the thermodynamics of constrained transformations, J. Mater. Sci. 17 (1) (1982) 225–234.
[6] F. Wakai, S. Sakaguchi, Y. Matsuno, Superplasticity of yttria-stabilized tetragonal ZrO_2 polycrystals, Adv. Ceram. Mater. 1 (1986) 259–263.

[7] A.J.A. Winnubst, M.M.R. Boutz, Superplastic deep drawing of tetragonal zirconia at 1160 °C, J. Eur. Ceram. Soc. 18 (14) (1998) 2101–2106.
[8] Y.J. He, L. Winnubst, A.J. Burggraaf, H. Verweij, P.G.T. van der Varst, H.G. de With, Grain-size dependence of sliding wear in tetragonal zirconia polycrystals, J. Am. Ceram. Soc. 79 (12) (1996) 3090–3096.
[9] H. Muto, A. Matsuda, M. Sakai, Superplastic joining of 3Y-TZP, J. Eur. Ceram. Soc. 26 (4–5) (2006) 379–384.
[10] S. Ran, L. Winnubst, D.H.A. Blank, H.R. Pasaribu, J.-W. Sloetjes, D.J. Schipper, Effect of microstructure on the tribological and mechanical properties of CuO-doped 3Y-TZP ceramics, J. Am. Ceram. Soc. 90 (9) (2007) 2747–2752.
[11] M.J. Mayo, J.R. Seidensticker, D.C. Hauge, A.H. Carim, Surface chemistry effects on the processing and superplastic properties of nanocrystalline oxide ceramics, Nanostruct. Mater. 11 (2) (1999) 271–282.
[12] D. Vollath, K.E. Sickafus, Synthesis of nanosized ceramic oxide powders by microwave plasma reactions, Nanostruct. Mater. 1 (5) (1992) 427–437.
[13] G.L. Messing, S.C. Zhang, G.V. Jayanthi, Ceramic powder synthesis by spray-pyrolysis, J. Am. Ceram. Soc. 76 (11) (1993) 2707–2726.
[14] G. Skandan, Processing of nanostructured zirconia ceramics, Nanostruct. Mater. 5 (2) (1995) 111–126.
[15] A.J.A. Winnubst, W.F.M. Groot Zevert, G.S.A.M. Theunissen, A.J. Burggraaf, Microstructure characteristics of ultra-fine ZrO_2–Y_2O_3 ceramic powders, Mater. Sci. Eng. A 109 (1989) 215–219.
[16] W.F.M. Groot Zevert, A.J.A. Winnubst, G.S.A.M. Theunissen, A.J. Burggraaf, Powder preparation and compaction behavior of fine-grained Y-TZP, J. Mater. Sci. 25 (8) (1990) 3449–3455.
[17] Y. Qin, Q. Zhang, Z.L. Cui, Effect of synthesis method of nanocopper catalysts on the morphologies of carbon nanofibers prepared by catalytic decomposition of acetylene, J. Catal. 233 (2) (2004) 389–394.
[18] N. Jongen, H. Hofmann, P. Bowen, J. Lemaitre, Calcination and morphological evolution of copper oxalate particles, J. Mater. Sci. Lett. 19 (12) (2000) 1073–1075.
[19] M.A.C.G. van de Graaf, J.H.H. ter Maat, A.J. Burggraaf, Microstructure and sintering kinetics of highly reactive ZrO_2–Y_2O_3 ceramics, J. Mater. Sci. 20 (5) (1985) 1407–1418.
[20] W.E. van Zyl, L. Winnubst, T.P. Raming, R. Schmuhl, H. Verweij, Synthesis and characterisation of dual-phase Y-TZP and RuO_2 nanopowders: dense electrode precursors, J. Mater. Chem. 12 (3) (2002) 708–713.
[21] M.A. Mohamed, E.K. Galwey, A kinetic and mechanistic study of the thermal-decomposition of copper (II) oxalate, Thermochim. Acta 217 (1993) 263–276.
[22] R.G. Avery, J.D.F. Ramsay, Sorption of nitrogen in porous compacts of silica and zirconia powders, J. Colloid Interface Sci. 42 (3) (1973) 597–606.
[23] R.G. Horn, Particle interactions in suspensions, in: R.A. Terpstra, P.P.A.C. Pex, A.H. de Vries (Eds.), Ceramic Processing, Chapman and Hall, London, 1975, pp. 58–101.
[24] J. Lyklema, Interfacial electrochemistry of disperse systems, in: R.F. Davis, H. Palmour, III, R.L. Porter (Eds.), Emergent Process Methods for High-Technology Ceramics, vol. 17, Plenum Press, New York, 1984, pp. 1–24.
[25] L. Winnubst, S. Ran, E.A. Speets, D.H.A. Blank, Analysis of reactions during sintering of CuO-doped 3Y-TZP nano-powder composites, J. Eur. Ceram. Soc. 29 (12) (2009) 2549–2557.